

# Correlation Analysis of Multiple-Input Multiple-Output Channels with Cross-Polarized Antennas

Lei Jiang, Volker Jungnickel, Stephan Jaeckel, Lars Thiele and Armin Brylka  
 Fraunhofer Institute for Telecommunications, Heinrich-Hertz-Institut  
 Einsteinufer 37, D-10587 Berlin, Germany  
 Email: lei.jiang@hhi.fraunhofer.de

**Abstract**—In this paper, we investigate the correlation characteristics of the multiple-input multiple-output (MIMO) channels based on the outdoor measurement. The correlation coefficients for both co-polarized and cross-polarized channels are studied. Results show that the polarization decorrelation performs better than spatial decorrelation in strong line of sight (LOS) scenario. In non line of sight (NLOS) scenario, they are of the same order. The envelope correlation coefficient is observed to be approximately the same as the power correlation coefficient in both time and frequency domain. The correlation of the channels highly depends on the propagation scenarios, and it increases as the Ricean  $K$  factor increases. It is also found that the correlation in the elevation domain is much higher than that in the azimuth domain.

## I. INTRODUCTION

The multiple-input multiple-output (MIMO) system has been shown to dramatically increase the capacity of the wireless system and it draws increasing attentions in recent years [1], [2]. An important condition for MIMO channels to achieve high capacity is that the environment provides sufficient multipath components. By exploiting the multipath components, the MIMO link results in a high rank channel with improved capacity. However, because of the correlation of the sub-channels, the rank of the channel may decrease in some propagation scenario such as LOS scenario. Therefore, efforts are paid to reduce the correlation of sub-channels, and techniques such as polarization are employed in the MIMO communication system. Thus it is of great interest to investigate the correlation characteristics of the MIMO channels.

[3] studied the correlation of the MIMO channels for indoor environment based on measurements. The spatial decorrelation has been analyzed for both transmitter and receiver. The joint advantage of spatial and polarization decorrelation was not given due to the limitation of the measurement. [4] investigated the cross correlation values for dual-polarised indoor MIMO links at 5.2 GHz. The measurement was made mainly in a NLOS corridor and hall scenario, and the correlation coefficients are calculated for differently polarized links and co-polarized array elements.

In this paper, we aim at analyzing the correlation characteristics of the MIMO channels for outdoor propagation environments. Based on the measurement at 2.53GHz, the channel correlation coefficients for both cross-polarized and co-polarized channels will be investigated in time and

frequency domain. Polarization and spatial decorrelation are compared, and the scenario dependency of the channel correlation is also analyzed. For spatial decorrelation, we further study the correlation coefficient in both azimuth and elevation domain.

## II. MEASUREMENT SETUP



Fig. 1. Transmit and receive antennas.

Measurements were made on the campus of Technical University Berlin (TUB) at 2.53 GHz with the RUSK HyEff channel sounder in a 20 MHz band. The base station is a uniform linear array (ULA) with cross-polarized patch antenna elements on it as shown in the top of Fig.1. The four patches in each column are coupled to narrow the beam width and hence obtain higher antenna gain. The left-most and right-most columns of array are grounded via 50  $\Omega$  resistor to minimize the edge effects. Therefore, altogether 8 columns of cross-polarized antennas at  $\lambda/2$  spacing, i.e., 16 transmit antennas are used as active elements. A +44 dBm power amplifier with a  $1 \times 16$  high power switch is used for the multiple antennas. The effective transmit power is +37 dBm per antenna, due to the 4 dB insertion loss of the switch and -3 dB antenna efficiency.

The noise figure of the HyEff receiver is 2.5 dB. Low-loss feeder cables are used to reduce receiver noise.

$$\rho^{env}(f_j) = \frac{\sum_i \left( |h_{mn}(f_j, t_i)| - \overline{|h_{mn}(f_j)|} \right) \left( |h_{m'n'}(f_j, t_i)| - \overline{|h_{m'n'}(f_j)|} \right)}{\sqrt{\sum_i \left| |h_{mn}(f_j, t_i)| - \overline{|h_{mn}(f_j)|} \right|^2 \sum_i \left| |h_{m'n'}(f_j, t_i)| - \overline{|h_{m'n'}(f_j)|} \right|^2}} \quad (2)$$

$$\rho^{env}(t_i) = \frac{\sum_j \left( |h_{mn}(f_j, t_i)| - \overline{|h_{mn}(t_i)|} \right) \left( |h_{m'n'}(f_j, t_i)| - \overline{|h_{m'n'}(t_i)|} \right)}{\sqrt{\sum_j \left| |h_{mn}(f_j, t_i)| - \overline{|h_{mn}(t_i)|} \right|^2 \sum_j \left| |h_{m'n'}(f_j, t_i)| - \overline{|h_{m'n'}(t_i)|} \right|^2}} \quad (3)$$

Altogether, the link margin is improved by almost 20 dB compared to [5].

All antennas are made of similar patch elements with two points of delivery feeding horizontal and vertical polarization. Cross-polarization coupling is smaller than -20 dB, measured back-to-back between two patches. The 3 dB antenna aperture is about  $90^\circ$  both in azimuth and elevation. The receivers are built in two forms. One is a cylinder with 8 cross-polarized patch antennas on the surface arranged in a row. The other is a cylindrical antenna made of two 12-patch elements arranged in two rows. On top a cube antenna is mounted as shown in the lower part of Fig.1.

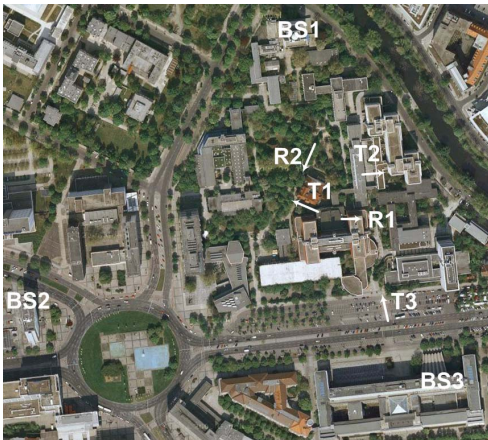


Fig. 2. Locations of the base station and terminal antennas.

The base station is mounted on the rooftop of the buildings indicated as BSx in Fig. 2, where BS1 is on Heinrich-Hertz-Institut (HHI), BS2 is on Deutsche Telekom (DTAG) and BS3 is on the main building of the TUB. The receiver sites marked with Rx use the cylindrical antenna as shown in the bottom left of Fig.1. Those marked with Tx use the antenna shown in the bottom right of Fig.1. The receiver is placed at the ground level for about 2 m high. Short tracks of 10 m inside campus area and long tracks with a total length of approximately 4.5 km outside the campus area were measured.

### III. CORRELATION COEFFICIENTS

For a series of  $n$  measurements of  $X$  and  $Y$ , the Pearson product-moment correlation coefficients can be used to

calculate the correlation of  $X$  and  $Y$ .

$$\rho = \frac{n \sum_i x_i y_i - \sum_i x_i \sum_i y_i}{\sqrt{\left( n \sum_i x_i^2 - \left( \sum_i x_i \right)^2 \right) \left( n \sum_i y_i^2 - \left( \sum_i y_i \right)^2 \right)}} \quad (1)$$

where  $x_i$  and  $y_i$  denote the measured samples.

In the measurements, we sampled the signal at a frequency of 320MHz over 20MHz bandwidth along the measuring track. The over sampled data are removed during the data processing. Hence the envelope correlation coefficient for two arbitrary channels  $h_{mn}(f_j, t_i)$  and  $h_{m'n'}(f_j, t_i)$  in both frequency and time domain are defined as in (2) and (3). Where  $m$  and  $m'$  denote different receive elements and  $n$  and  $n'$  denote different transmit elements. In (2)  $\overline{|h_{mn}(f_j)|}$  and  $\overline{|h_{m'n'}(f_j)|}$  are the sample mean values of the envelopes of channels  $h_{mn}(f_j, t_i)$  and  $h_{m'n'}(f_j, t_i)$  over the time instances. We evaluate the correlation coefficients over all the snapshots of a selected sub trajectory. In (3), the correlation is evaluated over the whole bandwidth.  $\overline{|h_{mn}(t_i)|}$  and  $\overline{|h_{m'n'}(t_i)|}$  are the sample mean values of the envelopes of channels in time domain with respect to the channel bandwidth.

Similar results can be obtained for the power correlation of the channels. (4) and (5) on the top of next page are the definitions of the power correlation coefficients of two arbitrary channels  $h_{mn}(f_j, t_i)$  and  $h_{m'n'}(f_j, t_i)$  in both frequency and time domain.

It has been shown in [6] in theory that, under certain assumptions,

$$\rho^{env} \approx \rho^{pow}. \quad (6)$$

In the following parts of our paper, we will validate this approximation with measurement data.

## IV. MEASUREMENT RESULTS

### A. Envelope and Power Correlation Coefficient

The envelope and power correlation coefficients versus the channel bandwidth and the sampling snapshots are plotted in Fig. 3 and Fig. 4 for strong LOS scenario and NLOS scenario. In Fig. 3, the measurement was taken along a track of 9.7 m in LOS scenario. We can see that the cross-polarized channels perform better than the co-polarized channels in LOS scenario. It can be observed that the envelope correlation coefficients are approximately

$$\rho^{pow}(f_j) = \frac{\sum_i \left( |h_{mn}(f_j, t_i)|^2 - \overline{|h_{mn}(f_j)|^2} \right) \left( |h_{m'n'}(f_j, t_i)|^2 - \overline{|h_{m'n'}(f_j)|^2} \right)}{\sqrt{\sum_i \left| |h_{mn}(f_j, t_i)|^2 - \overline{|h_{mn}(f_j)|^2} \right|^2 \sum_i \left| |h_{m'n'}(f_j, t_i)|^2 - \overline{|h_{m'n'}(f_j)|^2} \right|^2}} \quad (4)$$

$$\rho^{pow}(t_i) = \frac{\sum_j \left( |h_{mn}(f_j, t_i)|^2 - \overline{|h_{mn}(t_i)|^2} \right) \left( |h_{m'n'}(f_j, t_i)|^2 - \overline{|h_{m'n'}(t_i)|^2} \right)}{\sqrt{\sum_j \left| |h_{mn}(f_j, t_i)|^2 - \overline{|h_{mn}(t_i)|^2} \right|^2 \sum_j \left| |h_{m'n'}(f_j, t_i)|^2 - \overline{|h_{m'n'}(t_i)|^2} \right|^2}} \quad (5)$$

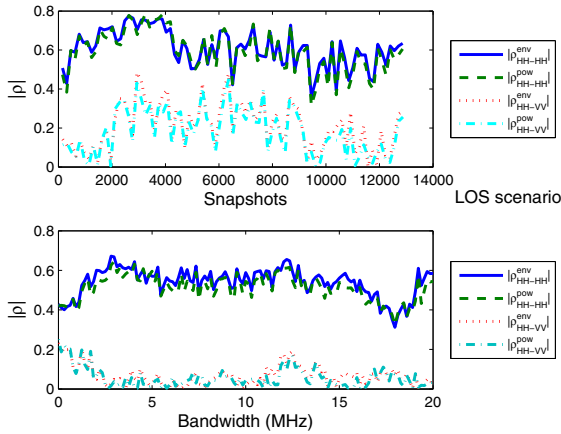


Fig. 3. The envelope and power correlation coefficients of co-polarized channels and cross-polarized channels in LOS scenario.

the same as the power correlation coefficients in both time and frequency domain, which validates the statement in [6]. Furthermore, from the figure we can also see that in the frequency domain, the correlation coefficients variations are relatively small, which means that the correlation coefficients are not very frequency selective in wideband transmission. In the measurement, we used a 20 MHz bandpass filter to smooth the channel. However, the channel correlation coefficients are highly time selective as shown in the top figure of Fig. 3, since the channel correlation depends on the propagation environment.

In the NLOS scenario, the channels are almost uncorrelated no matter using co-polarized antennas or cross-polarized antennas as shown in Fig. 4. The envelope correlation coefficients are also approximately equal to the power correlation coefficients. In this case, the dynamic range of correlation coefficients is also smaller in the frequency domain compared with that in the time domain.

In the following sections, we only consider the envelope correlation coefficients in the time domain for the simplicity of analysis.

### B. The Correlation Coefficients of Channels with Co-Polarized and Cross-Polarized Antennas

In our measurement, we used cross-polarized patch antennas as shown in Fig. 1, on which the vertically and horizontally polarized antennas are co-located. Therefore we are able to study the benefit due to polarization

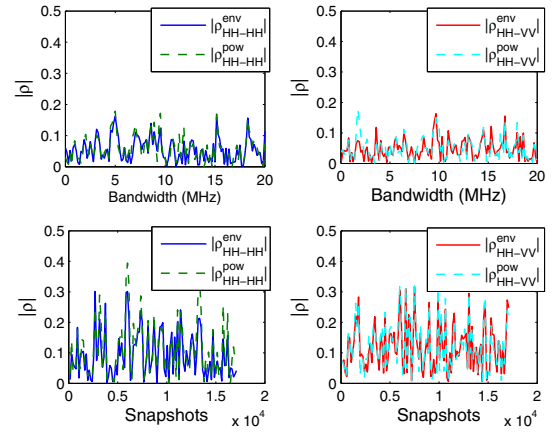


Fig. 4. The envelope and power correlation coefficients of co-polarized channels and cross-polarized channels in NLOS scenario.

decorrelation, which extends the results in [3]. Since here co-located antennas are used in the measurement, both spatial and polarization decorrelation can be investigated.

For MIMO channels with cross-polarized antennas, the channel matrix can be written as below

$$\mathbf{H} = \begin{bmatrix} \mathbf{H}_{VV} & \mathbf{H}_{VH} \\ \mathbf{H}_{HV} & \mathbf{H}_{HH} \end{bmatrix}. \quad (7)$$

To study the polarization decorrelation, we select one transmit antenna patch and one receive antenna patch, which give a  $2 \times 2$  MIMO channel, and check the correlation coefficient of the channel  $h_{VV}$  and  $h_{HH}$ , which is denoted by  $\rho_{HH-VV}$ . For the correlation of co-polarized channels, we actually take the spatial decorrelation into account, two neighboring patches at both the transmitter and receiver are chosen for analysis. The correlation coefficient is denoted by  $\rho_{HH-HH}$  or  $\rho_{VV-VV}$ , which represents the correlation coefficient of a  $2 \times 2$  MIMO channel with only horizontally or vertically polarized antennas.

The comparison between the correlation coefficients of the co-polarized and cross-polarized channels are plotted in Fig. 5. The evaluation is done in both strong LOS and NLOS propagation scenarios. It can be observed that the correlation of the channels are generally higher in LOS scenario than in NLOS scenario. In strong LOS scenario, when using co-polarized antennas arranged on two spatially separated patches, the probability of having correlation coefficient lower than 0.5 is less than 20%,

which means that the channels are highly correlated. With the use of cross-polarized antenna, 90% of the case the channels has correlation coefficient lower than 0.5, and 66% of the case, the correlation coefficient is lower than 0.3, where the channels can be considered as uncorrelated. This implicates that the polarization decorrelation works better than spatial decorrelation in LOS scenario. In NLOS scenario, 99% of the case the channels will have correlation coefficient lower than 0.5, and probability of having correlation coefficient lower than 0.3 is 90%. Therefore the channels in NLOS scenario can be approximated as independent from each other. In NLOS scenario, the cross-polarized antennas have no advantage with respect to polarization decorrelation since the polarizations have been destroyed by multiple reflections, diffractions or scattering during propagation.

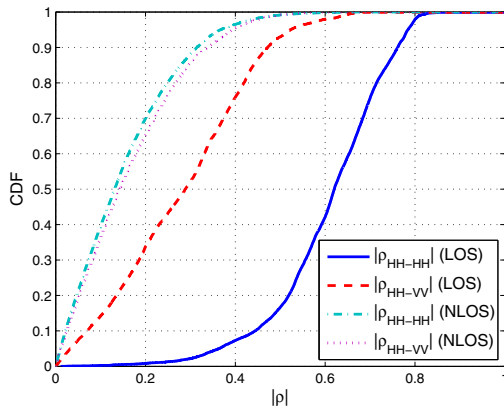


Fig. 5. The CDF of the absolute value of the correlation coefficients of channels with cross-polarized and co-polarized antennas.

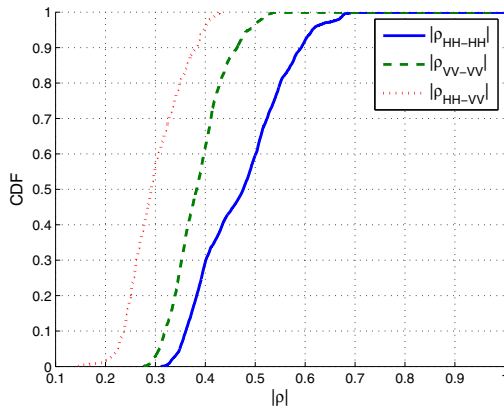


Fig. 6. The CDF of the mean values of  $|\rho|$  over all sub-channel pairs in LOS scenario.

In realistic communication systems, the performance of polarization decorrelation is affected by spatial decorrelation. Because of the cylinder geometry shape of the receive antenna as shown in the bottom of Fig. 1, even though the antenna is in LOS scenario, only one or two patches will have direct LOS component with the transmit antenna. For other antenna patches, the received signal mainly contains multipath components, especially those on the back side of the antenna (the front side is defined

as the side facing the transmit antenna). The effect of the polarization decorrelation in such case has been reduced, but the effect of spatial decorrelation increases. The CDF of the mean value of the channel correlation coefficients  $\rho$  over all sub-channel pairs is plotted in Fig. 6. It can be observed that, because of the spatial decorrelation, the average channel correlation is lower compared with Fig. 5. However, in general, the correlation of the cross-polarized channels is still smaller than that of the co-polarized channels. The cross-polarized channels are now affected by both the spatial and polarization decorrelation. Furthermore, the correlation of the vertically polarized channels is smaller than that of the horizontally polarized channels.

### C. Propagation Scenario Dependency

From the analysis above we know that the channel correlation coefficient highly depends on the propagation environment. In the top of Fig. 7, we plot the co-polarized channel correlation coefficients against the measuring distance along a longer track, which experiences different propagation scenarios. At the beginning of the track, the

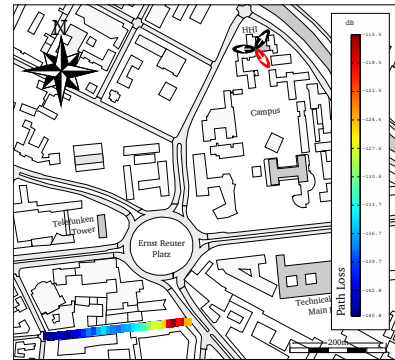
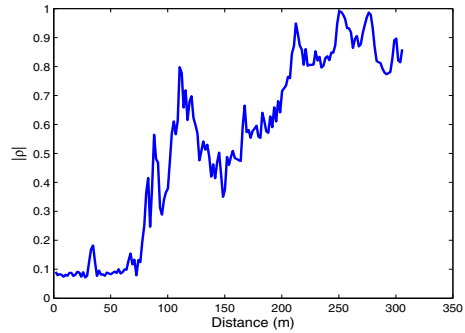


Fig. 7. The channel correlation coefficients and path loss measured along a track of 305 m.

receiver is in NLOS scenario to the base station, hence the channels are almost totally uncorrelated. As the receiver moves, it receives stronger and stronger signal, until it is in a weak LOS scenario. The path loss of the channel in dB is plotted in the bottom of Fig. 7. Since the different scenarios can be modeled using different Ricean  $K$  factors, we can come to the conclusion that the channel correlation coefficients increase along the measuring track as the Ricean  $K$  factor increases. The larger value at around 110

m is caused by the empty spacing between buildings as shown in the map of Fig. 7, where the shadow effect is weaker.

#### D. Correlation in the Azimuth and Elevation domain

In this section, we study the correlation of the channels in the azimuth and elevation domain. In the bottom right of Fig. 1, the antenna has two rows of receive patches on the cylinder surface. Therefore, we are able to investigate the correlation effects of the antennas in the same row (azimuth domain) or in the same column (elevation domain). The channel envelope correlation coefficients in

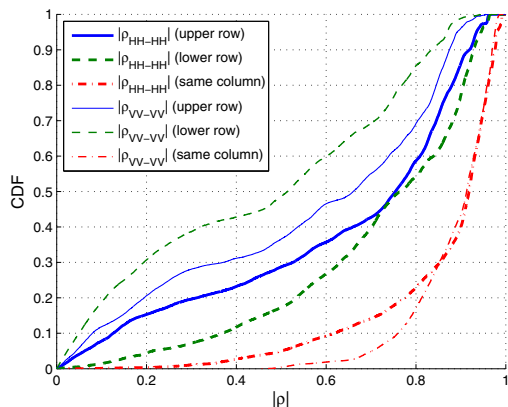


Fig. 8. The channel envelope correlation coefficients in LOS scenario.

LOS scenario is plotted in Fig. 8. From the figure we can see that the channel correlation in elevation domain is quite high no matter for vertically polarized or horizontally polarized channels. The correlation of the channels in azimuth domain is much lower, especially for the vertically polarized channels. This is consistent with the results in Fig. 6, where the correlation of the vertically polarized channels is lower than that of the horizontally polarized channels. Furthermore, it is also observed that the correlation for the horizontally polarized channels in the upper row is higher than that in the lower row. However, for the vertically polarized channels, the channels in the lower row have higher correlation.

#### V. CONCLUSION

We investigated the correlation of the MIMO channels with cross-polarized antennas for outdoor environment.

Results show that the polarization decorrelation performs better than the spatial decorrelation in LOS scenario, and the cross-polarized channels have smaller correlation coefficient than the co-polarized channels. Furthermore, the horizontally polarized channels tend to be more correlated than the vertically polarized channels. In both LOS and NLOS scenario, the envelope and power correlation coefficients are approximately the same. The correlation coefficients vary less in the frequency domain, but change dramatically in the time domain depending on the propagation environment where the channels undergo. It is also observed that, the correlation of the co-polarized channels increases as the Ricean  $K$  factor increases, and the channels have very high correlation in the elevation domain. In general, we can come to the conclusion that the cross-polarized channels are not affected by the environment, while the performance of the co-polarized channels is scenario dependent.

#### ACKNOWLEDGMENT

The authors would like to thank the German Ministry for Education and Research (BMBF) for the support in the projects 3GeT and EASY-C. The authors would also like to thank Udo Krüger, Thomas Wirth, Yosia Hadisusanto, Matthias Mehlhose, Stefan Schiffermüller and Kai Börner for preparing and performing the measurement. Efforts from Gerd Sommerkorn and Steffen Warzügel are also gratefully appreciated.

#### REFERENCES

- [1] M. A. Jensen and J. W. Wallace, "A review of antennas and propagation for MIMO wireless communications (invited paper)," *IEEE Trans. Antennas Propagat.*, vol. 52, pp. 2810–2824, Nov. 2004.
- [2] G. F. Foschini and M. J. Gans, "On limits of wireless communication in a fading environment when using multiple antennas," *Wireless Pers. Commun.*, vol. 6, no. 3, pp. 311–335, 1998.
- [3] P. Kyriatsi, D. C. Cox, R. A. Valenzuela, and P. W. Wolniansky, "Correlation analysis based on MIMO channel measurements in an indoor environment," *IEEE J. Select. Areas Commun.*, vol. 21, pp. 713–720, June 2003.
- [4] W. A. T. Kotterman, G. Sommerkorn, and R. Thoma, "Cross-correlation values for dual-polarised indoor MIMO links and realistic antenna elements," in *3rd International Symposium on Wireless Commun. Systems*, pp. 505–509, Sept. 2006.
- [5] V. Jungnickel, V. Pohl, H. Nguyen, U. Küger, T. Haustein, and C. von Helmolt, "High capacity antennas for MIMO radio systems," in *Proc. 5th WPMC*, vol. 2, pp. 407–411, 2002.
- [6] R. O. LaMaire and M. Zorzi, "Effect of correlation in diversity systems with Rayleigh fading, shadowing, and power capture," *IEEE J. Select. Areas Commun.*, vol. 14, pp. 449–460, Apr. 1996.